

## Electrochemical Behavior of Sodium Anions

Luis Montes<sup>†</sup> and J. J. Lagowski<sup>\*‡</sup>

Department of Chemistry, University of Central Oklahoma, Edmond, Oklahoma 73034, and Department of Chemistry and Biochemistry, The University of Texas at Austin, Austin, Texas 78712

Received: October 21, 2002; In Final Form: July 25, 2003

Electrochemical studies of sodium and its salts were carried out in 0.1 M TBAP and in electrolyte-free tetrahydrofuran solutions at room temperature. Working electrodes employed in these studies were platinum and mercury film ultramicroelectrodes, as well as a sodium electrode. The electrochemical reduction of sodium salts in 0.1 M TBAP/THF solutions leads to deposition of sodium on the platinum surface, and at more negative potentials, a stripping wave attributed to formation of the sodium anion is observed; the oxidation wave for the sodium anion is not observed. Possible mechanisms for the removal of the anion by competing processes are discussed. The results obtained from electrochemical studies of sodium electrodes and of sodium salts at a mercury film electrode are presented.

### Introduction

Our continuing interest in solutions of extremely reducing species has drawn us to solutions of alkali metal anions, specifically, their electrochemistry. The processes believed to give rise to solutions of the alkali metals in certain nonaqueous solvents are summarized<sup>1,2</sup> by eqs 1–3



The relative importance of these processes and the proportions of the corresponding species are affected by both the identity of the solvent and of the metal. Equilibria 2 and 3 are shifted far to the right in solvents that are strong solvators of cations and anions and which have relatively high dielectric constants, e.g., ammonia. For such solvents, the solvated electrons and metal cations are the predominant species; very low concentrations of the monomer species (M) and metal anions are also observed. However, all three equilibria are important in solvents such as hexamethylphosphamide (HMPA), methylamine (MA), and ethylenediamine (EDA); all of the species indicated in eqs 1–3 are present in such systems with the relative concentration of each being dependent on the identity of the alkali metal. The major anionic species produced is the metal anion, with only small concentrations of solvated electrons, in solvents such as the less polar amines and ethers, namely, ethylamine (EA) and tetrahydrofuran (THF). Relatively little electrochemical data has been reported concerning these species. Schindewolf has suggested that pulse radiolysis in conjunction with polarography could be used to obtain redox potentials for the metal anions.<sup>3</sup> Attempts have been made to study the sodium anion through the use of cyclic voltammetry, but these proved unsuccessful and have gone unreported in the open literature.<sup>4</sup> There have

been, however, a few reports of electrolysis studies, which provide further evidence for the existence of alkali metal anions. In a review of studies conducted on alkalides and electrides, Dye reported that, when solutions of  $(\text{Na}, \text{C}_{22})^+, \text{Na}^-$  in methylamine are subjected to DC electrolysis, sodium metal is deposited at the positive electrode, as expected for the oxidation of sodium anions to metallic sodium.<sup>1</sup> Other electrochemical work has involved emf studies of the thermodynamics of formation of various alkalide salts.<sup>4</sup>

The present study is focused on the electrochemical behavior of sodium analyte species. The sodium system may be the easiest system in which to electrochemically generate and/or observe alkali metal anions, because of the apparent stability of  $\text{Na}^-$  relative to the other alkali metal anions.<sup>1</sup> The potassium system, although presenting some interesting possibilities because of its somewhat anomalous behavior, has been the subject of a related study in this laboratory.<sup>5</sup> The rubidium and cesium systems were not studied because of the extreme reactivity of the metals. Also, the anions of these metals are reported to be the least stable of the alkali metals. The salts of these cations also tend to be the least soluble of the alkali metal salts in the nonaqueous solvents employed in this study. Some preliminary studies in these laboratories<sup>5</sup> involving lithium salts have still not yielded information on the existence of lithium anions. In the present study, the choice of the solvent, THF, was made based primarily on the particular state of the equilibria that exist in alkali metal solutions of this solvent.

### Experimental Section

The following electrolytes and alkali metal salts used in this study were ACS-reagent grade substances obtained from Aldrich Chemical Co., Inc. (Milwaukee, WI) and GFS (Columbus, OH): tetra-*n*-butylammonium perchlorate (TBAP), tetra-*n*-butylammonium hexafluorophosphate (TBA-PF<sub>6</sub>), tetra-*n*-butylammonium tetra-fluoroborate (TBA-BF<sub>4</sub>), tetra-*n*-butylammonium iodide (TBAI), NaClO<sub>4</sub>, and NaBr<sub>4</sub><sup>-</sup>. The electrolytes were dried under vacuum at 100 °C for at least 24 h prior to use. Alkali metal salts used as analytes (NaClO<sub>4</sub>, NaBF<sub>4</sub>), also ACS-reagent grade, were used as received from Aldrich; they were dried under vacuum for at least 24 h at 100 °C prior to use.

\* To whom correspondence should be addressed. E-mail: jjl@mail.cm.utexas.edu. Phone: 512/471-3288.

<sup>†</sup> University of Central Oklahoma.

<sup>‡</sup> The University of Texas at Austin.

Analyte samples of the alkali metals (Na, K) were obtained from Aldrich products using standard methods of dealing with reactive metals stored under oil. In some experiments, ferrocene (Fc) was used as an internal reference system. All electrolytes and analytes were stored in an argon-filled drybox (model HE-493, Vacuum Atmospheres Company, Hawthorne, CA). Dry tetrahydrofuran used as a solvent in these experiments was prepared from the Aldrich product using conventional techniques.

Electrochemical measurements were made with a model 273A Potentiostat/Galvanostat (EG&G Princeton Applied Research corporation) driven by a PARC model 270 Electrochemical Analysis System using software running on an IBM PS/2 model 55ST. The majority of the electrochemical experiments carried out in this study required the use of a supporting electrolyte and were carried out in a standard three-electrode glass cell. The cell contained an approximately 20-mL liquid well in which all measurements were made. In addition, two ground-glass joints were positioned on the walls of the cell above the well to allow addition of solid substances from glass dumpers.

The electrochemical cell was connected to a Schlenk line by a 9-mm (i.d.) O-ring joint. The cell could be opened to the Schlenk line through a high-vacuum stopcock equipped with O-rings. In three-electrode experiments, a platinum flag (approximately 1 cm<sup>2</sup>) was used as the counter electrode, and a coil of silver wire was used as a quasi-reference electrode (QRE). In experiments where a background electrolyte was not used, a two electrode arrangement was employed, following the example of Bonds et al.;<sup>6</sup> the silver wire quasi-reference electrode served as both reference and counter electrode in the two electrode arrangement.

The working electrodes employed in this study consisted of three types: polished platinum disk ultramicroelectrodes; mercury film on a platinum disk ultramicroelectrodes, and sodium disk electrodes. The procedure used to prepare the platinum electrode is similar to a procedure reported by Bonds et al.<sup>6</sup> The voltammetric responses of both types of platinum electrodes were checked by cyclic voltammetry in 0.5 M H<sub>2</sub>SO<sub>4</sub> to ensure the expected hydrogen adsorption waves were obtained.<sup>7,8</sup> Mercury film ultramicroelectrodes were prepared from platinum disk ultramicroelectrodes using a technique similar to that described by Baldo et al.<sup>9</sup>

In a typical experiment, baseline scans were recorded from +0.5 to -3.3 V versus the silver quasi-reference electrode at a sweep rate of 200 mV/s. Next, the analyte was added to the cell from the appropriate addition tube, and scans were recorded using the same electrochemical parameters as were used in baseline scans. After the electrochemical experiment was completed, ferrocene was added from the appropriate addition tube, and a cyclic voltammogram was again recorded. This procedure, using ferrocene as a reference redox system, permitted the comparison of electrochemical results between experiments.

## Results and Discussion

The primary focus of this work is the sodium system, although considerable information on the other alkali metals is available from our laboratories.<sup>5</sup> Some preliminary work for this study was conducted using ethylenediamine as a solvent; however, the bulk of the experiments described here were conducted in THF solutions, which, in our view, provide a number of experimental advantages over ethylenediamine. In most of our studies, tetrabutylammonium salts were used as supporting electrolytes. The bases of this choice are the very high cathodic

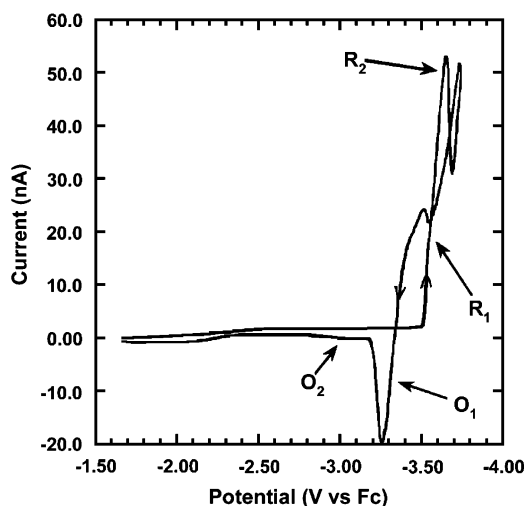


**Figure 1.** Cyclic voltammogram of 5 mM NaClO<sub>4</sub> in a solution of 0.1 M TBAP/THF, using a 25  $\mu$ m platinum ultramicroelectrode as the working electrode. Scan rate = 200 mV/s.

potentials that may be obtained using these kinds of electrolytic solutions, as well as the relatively high solubility of many tetrabutylammonium salts in THF. In some instances, we found it desirable to conduct electrochemical experiments in the absence of a supporting electrolyte, to determine the extent to which the electrolyte interferes with the alkali metal anions. In such cases, a platinum ultramicroelectrode was employed as the working electrode. The extremely small size of the electrodes helped to minimize the effects of solution resistance in THF.

**Platinum Electrodes.** The cyclic voltammograms of the sodium salts in 0.1 M TBAP/THF display quasi-reversible behavior at platinum working ultramicroelectrodes (Figure 1). Thus, for example, two reduction waves are observed on sweeping the potential from -1.7 to -3.75 versus the ferrocene reference redox couple for a 5 mM NaClO<sub>4</sub> solution in 0.1 M TBAP. The first electrochemical event is an inflection at -3.55 V (R<sub>1</sub>) followed by a wave (R<sub>2</sub>) that appears as a sharp, symmetric peak at -3.63 V, resembling a stripping peak.<sup>10</sup> On the return (anodic) scan, a cathodic wave occurs at -3.49 V, immediately after which, the current quickly falls, crossing the forward scan at -3.33 V, and leading to a very sharp, symmetric stripping wave (O<sub>1</sub>) at -3.26 V. On closer inspection, a much smaller oxidation wave (O<sub>2</sub>) is observed at -3.03 V.

The peak separation between the initial reduction wave (R<sub>1</sub>) and the main oxidation wave (O<sub>1</sub>) is 290 mV, much too large for an electrochemically reversible process. However, these two waves seem to be related because the oxidation wave only appears if the cathodic scan is carried to a sufficiently negative potential that includes at least the rising portion of the wave R<sub>1</sub>. Thus, assuming these two features are related, the system can be loosely described as electrochemically quasi-reversible, with kinetic factors effecting the magnitude of the separation.<sup>11</sup> Although there is little doubt that the second reduction event (R<sub>2</sub>) is a peak and resembles a stripping wave, the exact shape is difficult to determine because of its proximity to the cathodic limit.

Two series of experiments designed to provide an understanding of the effect of switching potential on the observed waves were conducted; the scan rate dependence of the waves were also determined. In the first series of experiments, the switching potential of the scan was progressively varied from a potential just negative of the nucleation overpotential to potentials just into the cathodic limit. The cathodic charge was recorded, from the point on the forward scan where the reverse

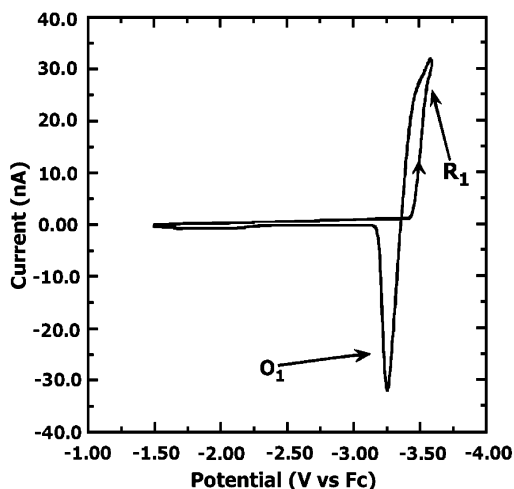


**Figure 2.** Cyclic voltammogram of 5 mM NaClO<sub>4</sub> in a solution of 0.1 M TBAP/THF using a 25  $\mu$ m platinum ultramicroelectrode, showing the nucleation loop and anodic stripping wave obtained for a switching potential of  $-3.60$  V. Scan rate = 200 mV/s.

scan crossed the forward scan to the same point on the reverse scan. The anodic charge associated with the sodium-stripping wave was also recorded, from the point where the anodic scan crossed the forward scan to the end of the stripping peak. The behavior of the various reduction and oxidation waves was also observed as the switching potentials were changed.

In the forward scan, Na<sup>+</sup> is reduced to Na<sup>0</sup> around  $-3.55$  V (Figure 1), the Na<sup>0</sup> being deposited on the surface of the Pt ultramicroelectrode. In the reverse (anodic) scan, the current is larger than in the forward scan in the region of  $-3.5$  to  $-3.35$ , which is indicative of depositing Na<sup>0</sup> on the electrode surface.

In studies of the switching-potential dependence of the anodic charge to the cathodic charge ( $Q_a/Q_c$ ) (vide infra), the anodic charge was close to equal to the cathodic charge in cases when the potential sweep was switched just prior to just after the current inflection in the forward scan. However, as the switching potential is shifted to more negative potentials, the ratio of anodic to cathodic charges decreases, indicating that not all of the Na<sup>0</sup> initially deposited on the electrode surface is available for oxidation because of the proximity of the cathodic stripping peak at  $-3.63$  V. If we are correct in our assignment of the sharp cathodic wave at  $-3.63$  V to the reduction of Na<sup>0</sup>, then this would effectively reduce (decrease) the amount of Na<sup>0</sup> on the platinum surface available for oxidation.

Another piece of evidence for the reduction of Na<sup>0</sup> to Na<sup>-</sup> is seen in the return scan in Figure 1; the current begins to decrease in a normal fashion. However, as the anodic sweep becomes more positive than the reduction of Na<sup>0</sup> to Na<sup>-</sup> and closer to the reduction of Na<sup>+</sup>, the current again begins to increase, producing the nucleation loop once again. The cathodic peak ( $-3.49$  V) in the anodic scan is a result of a sudden increase in the amount of sodium depositing on the electrode surface, presumably because of the loss of a competing sodium-removal process, indicating that the sharp stripping wave at  $-3.63$  V results from a process competing with the deposition of Na<sup>0</sup> on the electrode surface. The most likely process to remove Na<sup>0</sup> from the electrode surface in the forward scan is the reduction of Na<sup>0</sup> to sodide ions, Na<sup>-</sup>.

The scan rate chosen for these experiments was 200 mV/s, a rate that allowed us to observe both reduction waves in the forward scan. The main features observed in the switching potential study are summarized in Figure 2. Nucleation of the sodium phase on the platinum electrode occurs at  $-3.42$  V

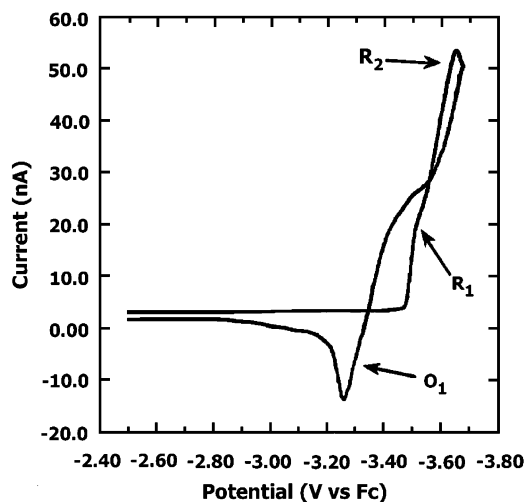


**Figure 3.** Cyclic voltammogram of 5 mM NaClO<sub>4</sub> in a solution of 0.1 M TBAP/THF using a 25  $\mu$ m platinum ultramicroelectrode, showing formation of the cathodic stripping wave. Scan rate = 200 mV/s.

during the forward scan. If the direction of the potential scan is reversed at a potential prior to, or during the current inflection, a nucleation loop is observed, with the anodic scan becoming higher than that for the cathodic scan (Figure 2). The reverse scan of this nucleation loop is immediately followed by a sharp anodic stripping peak at  $-3.26$  V. When the switching potential is no more than 30 mV beyond the deposition potential, the cathodic and anodic charges are almost equal.

A shift of the switching potential toward potentials more negative than the current plateau produces a second steep current increase and leads to the formation of a cathodic stripping peak at  $-3.63$  V (Figure 3). At slightly more negative potentials, the current decreases sharply, until the cathodic limit is reached at  $-3.69$  V. At switching potentials between the initial current plateau and the peak of the cathodic stripping wave, the nucleation loop for sodium deposition is still observed (Figure 2). However, if the switching potential is more negative than the peak potential of the second cathodic wave, a regular anodic current decrease is observed initially (Figure 3). As the reverse (anodic) scan reaches potentials less negative than the potential of the stripping peak, R<sub>2</sub>, the anodic current increases again, leading to a cathodic wave and the nucleation loop observed previously; the anodic stripping wave is again observed immediately following the nucleation loop. Furthermore, the anodic wave, O<sub>2</sub>, is occasionally observed if the forward scan is allowed to continue at least to the apex of the cathodic peak potential R<sub>2</sub>. The cathodic charge continues to increase proportionally with time from the deposition potential to the potential in the return scan when sodium begins to be oxidized. However, the charge associated with the anodic stripping peak (O<sub>1</sub>) increases only slightly over the same range, so that, although the ratio of the anodic to cathodic charge is approximately 0.4 when the switching potential is at R<sub>1</sub>, it decreases to about 0.2 by the time the switching potential is at the peak potential of R<sub>2</sub>.

The second set of studies involved observing the changes in the various reduction and oxidation waves as a function of scan rate, which was carried out by setting the switching potential at a value sufficiently negative to include the second reduction wave, typically about  $-3.8$  V. The sodium perchlorate system was studied at scan rates ranging from 0.02 to 5.4 V/s, and at a range of concentrations from 3.7 to 9.4 mM. The results, displayed in Figure 4, can be summarized as follows. As the scan rate is increased, the overpotential for sodium deposition shifted to more negative potentials, so that it varied by over



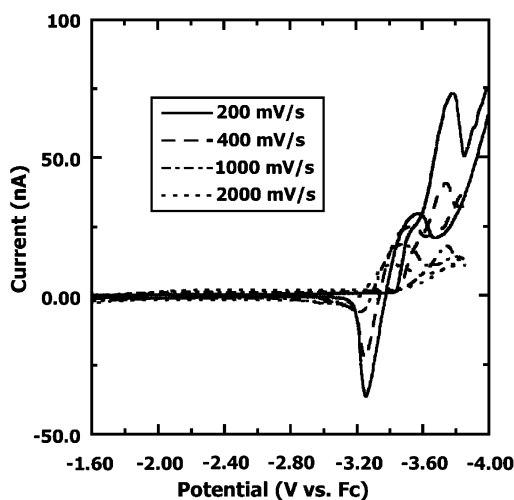


**Figure 4.** Scan rate dependence of the redox processes observed in the cyclic voltammogram of 0.5 M NaClO<sub>4</sub> in 0.1 M TBAP/THF. The working electrode was a 25  $\mu$ m diameter platinum ultramicroelectrode.

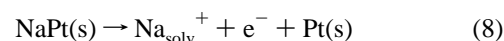
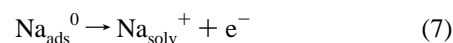
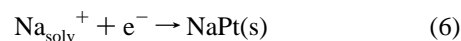
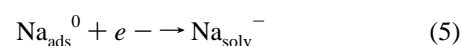
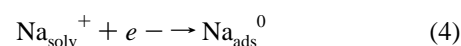
200 mV over the entire range of scan rates. The current increase at this point also exhibits a change in behavior; as the scan rate increases, the slope of the current increase became more gradual. However, the sharp cathodic wave, R<sub>2</sub>, remained at a relatively constant potential up to about 1.5 V/s, at which point it was lost in the current increase at the cathodic limit. The current associated with this wave also decreased and, at faster scan rates, the wave took on the appearance of a more rounded, diffusion controlled wave, rather than that of a sharp surface wave.

The anodic stripping wave also shifted to more positive potentials as the scan rate increased. As with the sharp cathodic wave, the anodic stripping wave exhibited a decrease in current and began to resemble a diffusion controlled wave. The magnitude of the potential shift for this wave also appeared to be concentration-dependent, with the 9.4 mM NaClO<sub>4</sub> solution yielding a shift of over 420 mV. However, at faster scan rates, the wave observed at -3.03 V (O<sub>2</sub>) maintained an approximately constant current, so that at faster scan rates, the ratio of the currents for O<sub>1</sub> compared to O<sub>2</sub> decreased. It is not clear how much of the potential shift of O<sub>1</sub> is due to a scan rate effect, as opposed to a decrease in the current associated with this wave and some overlap from the second oxidation wave, O<sub>2</sub>.

**Mercury Film Electrodes.** Our experiments suggested that sodium is strongly absorbed on platinum electrodes, a process that might be ameliorated at a mercury electrode with the formation of a sodium amalgam, NaHg<sub>x</sub>. The use of mercury electrodes should produce an anodic shift in the reduction of sodium cations. Indeed, it has been observed in some systems that the reduction of alkali metal cations at mercury electrodes can occur as much as one volt more positive than the corresponding reduction at solid electrodes.<sup>12</sup> Furthermore, the cathodic limit at mercury electrodes is often shifted to more negative potentials so that the Na<sup>+</sup> reduction event(s) should be well separated at the cathodic limit. Cyclic voltammograms using the complete suite of standard experiments on NaClO<sub>4</sub> and NaBF<sub>4</sub> in TBAP/THF solutions showed only quasi-reversible events (E<sub>pc</sub> = -2.55V and E<sub>pa</sub> = -2.37V vs Fc), which we attribute to the Na<sup>+</sup>/Na<sup>0</sup> couple. There is no evidence of further electrochemical behavior in either the forward or reverse scans.

**Electrochemical Processes.** The results of our experiments suggest that the electrochemical features that appear in the cyclic voltammogram of NaClO<sub>4</sub> in TBAP/THF solutions, Figure 1, can be described by eqs 4–8. The “inflection” at -3.55 V is

assigned to the reduction of Na<sup>+</sup> to Na<sup>0</sup> (eq 4)



Continuing the potential sweep up to this point is sufficient to obtain the corresponding anodic stripping wave (O<sub>1</sub>) assigned to the oxidation and removal of Na<sup>0</sup> to Na<sup>+</sup>. In cyclic voltammograms with the switching potential (vide infra) no more than 30 mV beyond the deposition potential, the cathodic and anodic charges are almost equal. The wave at -3.63 V is assigned to the reduction of Na<sup>0</sup> to Na<sup>-</sup> (eq 5). The wave is shaped more like a stripping wave, as would be expected of the reduction and removal of Na<sup>0</sup> from the electrode surface. The scan rate dependence of this wave is that expected of a stripping wave. Specifically, at faster scan rates, a decrease in current occurs, and it becomes broader in shape, more like a diffusion-controlled wave. This same scan rate-dependent behavior is observed for the stripping wave assigned to oxidation of the zerovalent sodium from the electrode surface (eq 7). The anodic reduction wave at -3.49 V corresponds to the deposition of sodium cations on the electrode surface. In the forward scan, the current increases sharply at about -3.42 V, so it should be expected that sodium cations are still being reduced in the return scan at a potential of -3.49 V. The wave at -3.26 V in the return scan is assigned to the removal of Na<sup>0</sup> from the electrode surface due to oxidation of Na<sup>0</sup> to Na<sup>+</sup> (eq 7). This sharp and well-defined wave resembles a stripping wave, rather than a diffusion controlled wave. The scan rate-dependent behavior of this wave also supports its assignment as a stripping wave. In the cyclic studies involving only the Na<sup>+</sup> reduction (at -3.55 V in the forward scan) and Na<sup>0</sup> oxidation (at -3.26 V in the reverse scan), the anodic and cathodic charges are close to equal. The small wave at -3.03 V is assigned to the oxidation of sodium metal from the NaPt intermetallic phase<sup>13</sup> on the electrode surface (eq 8).

The lack of an observable wave assigned to the oxidation of sodide (Na<sup>-</sup>) to Na<sup>0</sup> can be explained from two points of view. Any sodium anions formed should be expected to rapidly diffuse away from the electrode, because of their charge. Sodium anions are also known to react with TBA cations.<sup>14</sup> Sodium anions formed would react with the electrolyte cations present in the diffusion layer near the electrode, a process that would remove the anions from solution so that they are not present for oxidation.

**Effect of the Switching Potential.** The plot of the anodic charge versus the cathodic charge, obtained for the experiments designed to study the effect of the switching potential on the system, displays two regions (Figure 5). In the first region (below ~ 100nC cathodic charge), which corresponds to switching potentials between the deposition potential and R<sub>1</sub>, the plot is linear with a slope of about 0.5. In the second region corresponding to switching potentials beyond R<sub>1</sub>, the plot levels off and there is only a minimal change in the anodic charge at these more negative stripping potentials. This type of behavior is expected for a process in which deposition of an electroactive species is followed by the electrochemical removal of the

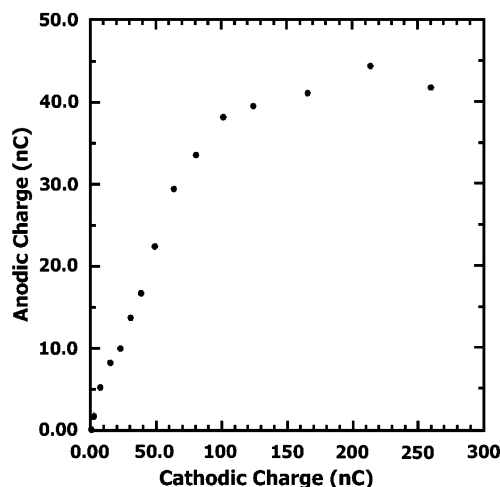


**Figure 5.** Plot of the anodic charge versus the cathodic charge for a cyclic voltammogram of 5 mM NaClO<sub>4</sub> in 0.1 M TBAP/THF. The working electrode was a 25  $\mu$ m diameter platinum ultramicroelectrode. Scan rate = 200 mV/s.

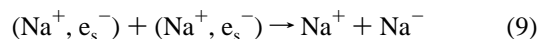
deposited species at slightly more negative potentials. At switching potentials close to the deposition potential, the primary electrochemical process is the reduction of the sodium cations to the metal; the anodic charge is almost equal to the cathodic charge because there are no competing processes to remove the sodium metal from the platinum surface. As the switching potential becomes more negative, cathodic stripping of the deposited sodium begins to take place, a process which removes sodium from the working electrode. At these negative potentials, sodium metal is still being deposited on the electrode (from Na<sup>+</sup>) and, indeed, this process will continue in the reverse scan until anodic oxidation of deposited sodium begins. Thus, the anodic stripping charge observed in the reverse scan is limited by the amount of sodium deposited on the electrode surface by the cathodic process in the reverse scan and it is not expected to be equal to the cathodic charge arising from the initial deposition of sodium in the forward scan. The rather complex behavior observed in this portion of the potential window makes it difficult to quantify relationships. The anodic stripping charge is never close to the cathodic charge when the switching potential is more than 40 mV beyond the deposition potential because the deposited sodium is removed by formation of sodium anions. We might expect to observe a wave corresponding to the oxidation of sodium anions unless these species are involved in a rapid reaction with another substance present in the solution; no obvious oxidation wave is observed prior to O<sub>1</sub>.

If the electrochemical process is simply that represented by eq 4, with the deposited sodium strongly adsorbed, adsorption peaks should be observed anodically of both the reduction and oxidation diffusion-controlled peaks. Although the current for R<sub>2</sub> decreases as the scan rate increases, the wave, R<sub>1</sub>, completely disappears. Furthermore, no potential shift is observed for R<sub>2</sub>, in either the anodic or cathodic direction. In addition, R<sub>1</sub> always has a much greater peak current than O<sub>2</sub> and, indeed, O<sub>2</sub> is not always observed. If both of these waves were associated with adsorption phenomena, they would be expected to have similar peak currents.<sup>15</sup> Thus, it appears that the voltammetric behavior observed cannot be described as simply reduction of sodium cations with adsorption of sodium metal.

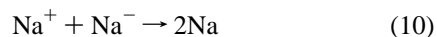
The observed electrochemical behavior could be the result of the combined reactions described in eqs 4 and 5, that is, deposition of sodium followed by cathodic stripping to form

the anions. However, some prewave should still be observed for this model of the observed behavior. It is unclear from the data that a prewave more positive than R<sub>1</sub> is present. In some scans, a very slight current increase is observed prior to this wave, which does not appear to be affected by increasing the scan rate. Possible prewave activity is difficult to observe because of the greater currents associated with the other cathodic processes. On the other hand, O<sub>2</sub> does behave somewhat like an adsorption wave for O<sub>1</sub>, in that the ratio of peak currents (O<sub>2</sub>/O<sub>1</sub>) increases with increasing scan rates. This interpretation assigns R<sub>1</sub> to the reduction process described by eq 4; R<sub>2</sub> then corresponds to the process corresponding to eq 5, the reduction of Na<sup>0</sup> to Na<sup>-</sup> with the anions produced rapidly diffusing away from the electrode. We would then expect an oxidation wave corresponding to the reverse process shown as eq 5; however, no corresponding oxidation wave is observed. In this model, two questions arise; the origin of the sodium removed by O<sub>1</sub> and the reason for the absence of a wave corresponding to oxidation of Na<sup>-</sup>.

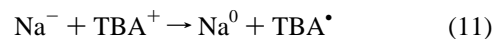
The first of these questions is easily answered. In the forward scan, reduction of sodium cations continues to occur as deposited sodium is reduced to Na<sup>-</sup>. Then, in the return scan, at potentials that are no longer sufficiently negative to support generation of the anions, the reduction of sodium cations continues. Thus, a sodium layer will still be present on the electrode as the reverse scan reaches potentials at which sodium is oxidized and the anodic stripping wave is observed. However, the lack of a sodium anion oxidation wave must still be addressed. The absence of a Na<sup>-</sup> oxidation wave is consistent with the chemical removal of that species. Fletcher and colleagues have shown, through pulse radiolysis studies of dilute metal or sodium salt solutions in THF, that cation-solvated electron ion pairs formed can react to produce both the cation and the anion, according to eq 9<sup>16</sup> which was shown to be an



important process in the generation of sodium anions. On the other hand, the reverse reaction was not a significant pathway for removal of anions from the solution.<sup>11</sup> Rather, the anions were destroyed by reaction with radiolytically produced radicals. If, in the present study, any sodium anion species produced were destroyed by reaction with another species, two possible reaction partners exist. One is the sodium cation (eq 10), which should be present in relatively high concentrations in the diffusion



layer at these very negative potentials. It is also possible that the presence of the tetrabutylammonium cations is enough to remove any sodium anions produced (eq 11)



Dye reports<sup>4</sup> that attempts to make tetra-alkylammonium sodide results in an irreversible decomposition process. Thus, Na<sup>-</sup> could be scavenged by the supporting electrolyte cation in our experiments. Provided that the rate of such a reaction is fast on the voltammetric time scale, the removal of sodium anions in this manner would then account for the inability to observe a wave corresponding to electrochemical oxidation of the anionic species.

**Other Routes to the Production of Sodium Anions.** Other methods were also attempted to generate sodium anions in THF electrochemically. Because sodium is insoluble in THF, it should

be possible to use a sodium electrode as the working electrode, which would be stable to dissolution at the rest potential, and we expected that sodium could be directly reduced to produce the anions in THF.

Although sodium electrodes were produced successfully, several attempts to generate sodium anions with these electrodes did not produce the desired results. The rest potential of the sodium electrode in 0.1 M solutions of TBAP in THF is  $-3.0$  V versus the silver wire quasi-reference electrode. If the sodium electrode were not electrochemically treated prior to use, voltammograms recorded from the rest potential to  $-4.0$  versus the rest potential displayed sloping lines, with no other obvious features. However, if the electrode was first held for about five minutes at a potential much more positive than the rest potential, small cathodic features, possibly corresponding to reduction of  $\text{Na}^+$ , were observed when the potential was scanned from  $+1.0$  V to  $-3.0$  V versus the rest potential. A blue color, which would be indicative of the presence of the metal anions (or solvated electrons), was never observed during the electrolysis. The sodium electrode was also studied in dilute (3–13 mM) solutions of sodium perchlorate, but the high resistivity of these solutions and the relatively large size of the electrode prevented the observation of any clear oxidative or reductive behavior.

In a few experiments, the liquid NaK alloy was used as the analyte in solutions of 0.1 M TBAP in THF. The alloy was chosen as an analyte because of its well-known ability to produce sodium anions in THF.<sup>1,17</sup> Indeed, it has been reported that the alloy will produce sodium anions preferentially in THF, although not to the complete exclusion of potassium anions.<sup>16</sup> With the alloy as analyte, the only electrochemical activity observed using a mercury film electrode involved redox processes associated with the  $\text{K}^+/\text{K}^0$  couple. In addition, a coating formed on the liquid alloy surface and the solution became cloudy during these experiments. The surface deposit and precipitate may be the product of a reaction between the alloy and the electrolyte. In solutions of the alloy in pure THF, neither the coating nor the precipitate is observed. Given the very low solubility of potassium salts in THF, the precipitate is most likely a result of the formation of a relatively insoluble salt from the  $\text{K}^+$  produced by the alloy and the electrolyte anion,  $\text{ClO}_4^-$ . Similar observations were made using other tetra-*n*-butylammonium electrolytes with the only difference being the concentration of free potassium ions in solution observed by cyclic voltammetry. Once again, however, no electrochemical behavior was observed that could be attributed to either sodium or potassium anionic species.

Finally, attempts were made to study the sodium perchlorate system in THF without the presence of an added electrolyte by using platinum ultramicroelectrodes. The concentrations of sodium perchlorate used were in the range of 2–9 mM. Scan rates used in these studies ranged from 50 to 500 mV/s. In these studies, a flat current response was obtained over most of the potential window.

## Conclusions

The most promising results were obtained from studies of sodium salts at platinum ultramicroelectrodes. The first reduction

wave and nucleation loop are attributed to the reduction of sodium cations and subsequent deposition on the platinum electrode. The prominent oxidation wave observed in the return scan is assigned to the anodic stripping of the deposited sodium from the electrode to regenerate sodium cations. A second reduction wave is also observed in the cathodic scan, and assignment of this wave is more problematic. The best available data suggest that this wave is the result of cathodic stripping of sodium from the electrode to produce sodium anions. However, the usual detailed analysis of this wave is hindered by its proximity to the rapidly increasing current at the cathodic limit.

The results of sodium studies at mercury film electrodes are less promising in terms of the possibility of generating, or even observing, sodium anions in this system. Although the reduction and oxidation waves observed for the  $\text{Na}^+/\text{Na}^0$  couple are well characterized and, for the most part, agree with the previous reports, there is no electrochemical evidence for sodium anions in this system. Indeed, the extra stability associated with the sodium amalgam may result in a cathodic shift of the potential for electrochemical generation of sodium anions, so that this process occurs at potentials more negative than the cathodic limit of the system studied.

**Acknowledgment.** We gratefully acknowledge the generous support of the Robert A. Welch Foundation.

## References and Notes

- (1) Dye, J. L. *Prog. Inorg. Chem.* **1982**, 32, 329–441.
- (2) Dye, J. L. *J. Chem. Educ.* **1977**, 54, 332–339.
- (3) Schindewolf, U. comment in the general discussion following: Fletcher, J. W.; Seddon, W. A. *J. Phys. Chem.* **1975**, 79, 3055–3064.
- (4) Dye, J. L., private communication.
- (5) Montes, L. D. Ph.D. Dissertation, The University of Texas at Austin, 1996.
- (6) Bonds, A. M.; Fleischman, M.; Robinson, J. J. *Electroanal. Chem.* **1984**, 168, 299–312.
- (7) (a) Inocencio, A. A. *J. Electrochim. Acta* **1978**, 23, 977–981. (b) Dye, J. L., private communication.
- (8) Koppang, M. D.; Holme, T. A. *J. Chem. Educ.* **1992**, 69, 770–773. Scarr, R. F. In *Encyclopedia of the Electrochemistry of the Elements*; Bard, A. J. Ed.; Marcel Dekker: New York, 1986; Vol. 9, Part B.
- (9) Danielle, S.; Baldo, M. A.; Corbette, M.; Mazzocchin, G. A. *J. Electroanal. Chem.* **1994**, 379, 261–270.
- (10) (a) Shain, I. In *Treatise on Analytical Chemistry*; Kolthoff, I. M., Elving, P. J., Eds.; Interscience: New York, 1978; Part I, Vol. 4, Chapter 50. (b) Nicholson, M. M. *J. Am. Chem. Soc.* **1959**, 79, 7.
- (11) Bard, Allen J.; Faulkner, Larry R. *Electrochemical Methods: Fundamentals and Applications*; Wiley: New York, 2001.
- (12) Scarr, R. F. In *Encyclopedia of the Electrochemistry of the Elements*; Bard, A. J., Ed.; Vol. 9, Part B, Marcel Dekker: New York, 1986.
- (13) *Binary Alloy Phase Diagrams*; Massalski, T. B., Ed.; American Society for Metals: Metals Park, Ohio, 1986.
- (14) Concepcion, R.; Dye, J. L. *J. Am. Chem. Soc.* **1987**, 109, 7203–7204.
- (15) Wopscall, R. H.; Shain, I. *Anal. Chem.* **1967**, 39, 1514–1527.
- (16) Salmon, G. A.; Seddon, W. A.; Fletcher, J. W. *Can. J. Chem.* **1974**, 52, 3259–3268.
- (17) Dye, J. L. *Angew. Chem., Int. Ed. Engl.* **1979**, 18, 587–98.